Solid-State Electronics Vol. 35, No. 11, pp. 1585–1596, 1992
Printed in Great Britain.

0038-1101/92 $5.00 + 0.00

A MODEL FOR THE FIELD AND TEMPERATURE DEPENDENCE OF SHOCKLEY–READ–HALL LIFETIMES IN SILICON

A. SCHENK
Swiss Federal Institute of Technology, Integrated Systems Laboratory, Gloriastrasse 35, CH-8092 Zürich, Switzerland

(Received 9 March 1992; in revised form 22 May 1992)

Abstract—We derive a simple analytical model for the field and temperature dependence of Shockley–Read–Hall lifetimes in silicon from a microscopic level, where the capture of carriers at recombination centers is assumed to be a multiphonon process. Strong electric fields, as often present in modern devices, cause trap assisted tunneling, i.e. the multiphonon recombination path is no longer purely vertical in a band diagram, but has a horizontal branch at an effective energy which is given by the maximum of the transition probability. Applying reasonable approximations we calculate this effective recombination path as a function of field strength and temperature. Field enhancement factors of the inverse carrier lifetimes are then presented that require no integration, iteration or higher mathematical functions. The anisotropy and multi-valley nature of the silicon conduction band is carefully taken into account. We discuss all approximations and physical effects by means of the gold acceptor level. The model is able to describe the pre-breakdown behaviour of trap tunneling leakage and is suitable for the implementation into simulation packages.

NOTATION

Ai, Ai'	Airy function and its derivative
$c_n(x)$, $c_p(x)$	electron and hole capture rates ($cm^3 s^{-1}$)
E	energy (eV)
$E_{act}(F)$, E^0_{act}	activation energy for capture with and without electric field, resp. (eV)
E_c, E_v	conduction and valence band edges, resp. (eV)
$E_{F,n}$, $E_{F,p}$	quasi Fermi levels of electrons and holes, resp. (eV)
E_t	energy level of the recombination center (eV)
E_0, E_0^0	transition energy with and without electric field, resp. (eV)
$F(x)$	field strength ($V cm^{-1}$)
$F_i(x)$	ith component of the field strength ($V cm^{-1}$)
$\mathcal{F}$	electrooptical function $\mathcal{F}(y) = \mathrm{Ai}'^2(y) - y\mathrm{Ai}^2(y)$
f_B	Bose function
$f_{c,v}$	electron and hole distribution functions, resp.
$f_{t,n}$, $f_{t,p}$	trap occupation probabilities
$g_{c,n}$, $\tilde{g}_{c,n}$	field enhancement factors for electron and hole lifetimes, resp.
$g_{0,n}$, $g_{1,n}$	degeneracy factors of the recombination center for empty and occupied state, resp.
$\hbar\omega_0$	effective phonon energy (eV)
$\hbar\Theta_{i,\parallel}$, $\hbar\Theta_v$	electrooptical energies for electron and hole tunneling, resp. (eV)
I_l	modified Bessel function of order l
k	Boltzmann constant
l	number of phonons
M_c, M_v	multiphonon transition probabilities for electron and hole capture, resp.
$m_{i,\parallel}$	electron tunneling mass in field direction
m_t, m_l	transverse and longitudinal effective masses of electrons, resp.
m_v	effective hole mass
$N_t(x)$	concentration profile of the recombination centers (cm^{-3})
n, p	electron density, hole density (cm^{-3})
n_i	intrinsic density (cm^{-3})
n_1, p_1	electron and hole density of a nondegenerate semiconductor, if the Fermi level coincides with the trap level (apart from a degeneracy factor) (cm^{-3})
S^{SRH}_{net}	net Shockley–Read–Hall recombination rate ($cm^{-3} s^{-1}$)
S	Huang–Rhys factor
T	absolute temperature (K)
$\mathcal{T}_c$, $\mathcal{T}_v$	bound-to-band tunneling probabilities for electrons and holes, resp.
$W(E)$	thermal weight function
ϵ_F	combined energy determining E_0 (eV)
ϵ_R	lattice relaxation energy (eV)
ρ_c^0, ρ_v^0	dimensionless zero-field densities of band states for conduction and valence band, resp.
τ_v, $\tau_{v,0}$, $\tilde{\tau}_v(x)$	SRH lifetimes ($v = n$ electrons, $v = p$ holes) (s)

1. INTRODUCTION

Shockley–Read–Hall (SRH) and phonon-assisted band-to-band Auger recombination are the two important recombination processes in silicon. For non-degenerately doped material the SRH mechanism is generally dominant, and therefore, controls the carrier lifetime. High doping concentrations in modern devices not only favour Auger recombination, but also cause tunneling generation (reverse bias) and tunneling recombination (forward bias) in regions of sufficient large field strength. Tunneling transitions in the bulk are either phonon-assisted band-to-band or trap assisted (bound-to-band). Whereas the former are of second order due to the indirect gap, the latter are of first order because of the strong localization of

the bound state, but require a noticeable density of recombination centers in order to yield a macroscopic effect. From a quantum mechanical point of view there is no reason to consider trap-assisted tunneling independent from SRH recombination. The thermal capture and emission of carriers are enhanced by the field, since tunnel transitions at an energy below the thermal barrier height occur—in the extreme case at the trap level itself (pure trap tunneling). Thus, tunneling results in an effective lowering of the thermal barrier. On the other hand, the same process can be explained in terms of phonon-assisted bound-to-band tunneling, the only difference being the transition inducing interaction operator used. The concept of field-enhanced multiphonon transitions (induced by electron–phonon coupling) seems to be more realistic for silicon even at the operating temperature of liquid nitrogen (LN_2). This leads to the picture of field dependent SRH lifetimes, which are no longer constant in the device. A theory, based on the microscopic process of multiphonon recombination, was outlined in [1].

Experimentally, strong evidence for tunnel leakage currents in MOSFETs, trench DRAMs and bipolar transistors was found in recent years. An anomalously high non-ideal base current in forward-bias at LN_2 was reported by Woo *et al.*[2]. Del Alamo *et al.*[3] investigated bipolar devices with a base donor level ranging from 8.8×10^{17} to $4.0 \times 10^{19}\,\mathrm{cm}^{-3}$. Forward I–V curves of the p^{2+}–n^{+} emitter-base junctions showed a strong, exponential-like increase in the current at room temperature as the base doping level was raised beyond $\approx 5 \times 10^{18}\,\mathrm{cm}^{-3}$. The observed effect could be fitted with a simple tunneling expression which did not allow, however, to distinguish between interband and trap-assisted tunneling. Hurkx *et al.*[4] also observed an anomalous reduced temperature dependence and increased non-ideality factors in the temperature range from 77 to 300 K with an inverse dependence of the non-ideality factor on temperature. To describe the trap tunneling effect, they introduced "enlarged (field dependent) carrier concentrations" and field enhancement factors for the intrinsic densities into the SRH formula. The latter were adopted from Vincent *et al.*[5]. A better model was suggested by Voldman *et al.*[6]. They extracted field enhancement factors from the inverse carrier lifetimes in accordance with a strict theory. Various models of bound-to-band tunneling then were applied to explain the p^{+}-doped gate-diode leakage in planar MOSFETs.

In this paper we develop the theory of field enhanced multiphonon recombination (see [1]) to a simplified model of field-dependent SRH lifetimes. All approximations will be discussed together with the resulting limitations of the validity range of the model. In Section 2 we derive general expressions for the field enhancement factors. Using the high and low temperature approximations of multiphonon theory, these expressions are transformed then in Section 3 in such a way that no integrations, iterations or higher mathematical functions are necessary. Section 4 is devoted to the temperature dependence of zero-field lifetimes. We discuss the results in Section 5.

2. FIELD ENHANCEMENT FACTORS FOR THE LIFETIMES

We assume single-level recombination centers with a concentration $N_t(x)$ and (thermal) binding energy E_t measured from the conduction band minimum. The level $E_c(x) - E_t$ will be used as energy zero in the following. We neglect a possible Poole–Frenkel effect, i.e. the lowering of the Coulombic barrier tail in a strong electric field, if the deep center is charged[8]. We experienced that in a SRH model including trap tunneling the Poole–Frenkel effect can be absorbed by minor changes in the model parameters, because at strong fields the dominant recombination paths are deeper in the gap, where the barrier width is only little affected by the Coulomb potential. Nevertheless, the bound state field effect (Poole–Frenkel effect) can dominate the field dependence at lower field strengths.

The net rate of recombination at those centers is given by the well known SRH formula[7]

$$R_{\mathrm{net}}^{\mathrm{SRH}}(x) = \frac{np\left\{1 - \exp\left[-\dfrac{E_{\mathrm{F},n} - E_{\mathrm{F},p}}{kT}\right]\right\}}{\hat{\tau}_p(x)\dfrac{n}{f_{\mathrm{t},n}} + \hat{\tau}_n(x)\dfrac{p}{(1-f_{\mathrm{t},p})}}, \qquad (1)$$

where $E_{F,n} - E_{F,p}$ is the difference of the quasi Fermi potentials, and $f_t^{n,p}$ are the trap occupation probabilities

$$f_{\mathrm{t},\nu} = \left[1 + \frac{g_{0,\nu}}{g_{1,\nu}} \exp\left\{\frac{E_c - E_t - E_{\mathrm{F},\nu}}{kT}\right\}\right]^{-1} \qquad (2)$$

($g_{0,1}$-degeneracy factors of the empty and occupied trap level, respectively). Equation (1) holds for Fermi statistics. In the following we will restrict ourselves to the Boltzmann case. Furthermore, we replace the degeneracy factors by unity. With the usual definitions

$$n_1 = n(f_{\mathrm{t},n}^{-1} - 1), \quad p_1 = p(f_{\mathrm{t},p}^{-1} - 1)^{-1} \qquad (3)$$

eqn (1) then turns to the more familiar form

$$R_{\mathrm{net}}^{\mathrm{SRH}} = \frac{np - n_i^2}{\hat{\tau}_p(x)[n + n_1] + \hat{\tau}_n(x)[p + p_1]}. \qquad (4)$$

The $\hat{\tau}_\nu(x)$ are called SRH lifetimes

$$\hat{\tau}_n(x) = [c_n(x)N_t(x)]^{-1}, \quad \hat{\tau}_p(x) = [c_p(x)N_t(x)]^{-1}. \qquad (5)$$

Aside from the density of recombination centers they depend on the capture rates $c_{n,p}(x)$. The whole information about field and temperature dependence of the lifetimes is contained in these capture rates.

The rate eqn (1) is not based on any concrete capture mechanism, but only on the occupation statistics of electrons and holes. A theory for the lifetimes requires the process of energy transfer to be specified. Various mechanisms are possible: radiative,

Auger, cascade, plasmon interaction, defect reactions and so on. Probably the most important and most often met case is the nonradiative multiphonon recombination, where the electronic energy is transferred into lattice vibrations. Since the gap of silicon is much larger than the largest phonon energy, the capture of a carrier will be accompanied by the emission of many phonons. Only those centers which localize the captured carrier to a few elementary cells are capable for a sufficient strong electron–phonon coupling, which on the other hand is the precondition for multiphonon transitions. In silicon this strong localization of the deep level wave function has the favourable effect that no additional collision partner is necessary in any kind of SRH process (including bound-to-band tunneling), since the strong localization in real space causes a sufficient spread of the wave function in k-space. Therefore, off-diagonal matrix elements are first order quantities.

The microscopic description of field dependent capture rates $c_{n,p}(x)$ is based both on standard multiphonon theory[9–18] and on the theory of Bloch electrons in a strong electric field[19–34]. If these theories are combined[35,36], one obtains a theory of phonon-assisted trap tunneling, or field-enhanced multiphonon recombination, depending on whether the electric field or the electron–phonon coupling is considered the transition inducing force. This differentiation becomes important, when approximations of the general expressions are to be found. One can show for deep centers in silicon at room temperature[37] that at least in the pre-breakdown range the capture should be essentially a multiphonon process, i.e. phonon-induced and accompanied by the emission of some phonons. Hence, pure trap tunneling (horizontal path without phonon assistance) is rather unlikely.

The theory of field dependent lifetimes was outlined in [1] allowing for inhomogeneous fields. Here we should get rid of all complications in order to achieve a tractable expression for the purpose of device simulation. Therefore, the electric field is considered constant over a distance of the order of an interband tunnel length around the trap. Together with the above mentioned assumption that enough phonons are emitted during the capture, the restriction to the constant field approximation enables the necessary simplifications that will be discussed below.

As shown in [1], the inverse SRH lifetimes are given by

$$\hat{\tau}_n^{-1}(x) = \tau_{n,0}^{-1} N_t(x) \frac{1}{n} \sum_{l \geq 0} \rho_c^0(l) f_c(l) \mathcal{T}_c(l, x) M_c(l), \quad (6)$$

$$\hat{\tau}_p^{-1}(x) = \tau_{p,0}^{-1} N_t(x) \frac{1}{p} \times \sum_{l \geq 0} \rho_v^0(l)[1 - f_v(l)] \mathcal{T}_v(l, x) M_v(l). \quad (7)$$

Here, $f_{c,v}(l)$ denote the electron distribution functions for conduction and valence band, $\rho_{c,v}^0(l)$ are dimensionless zero-field densities of band states, $\mathcal{T}_{c,v}(l, x)$ is the bound-to-band tunneling probability, and $M_{c,v}(l)$ the multiphonon transition probability. The average is performed by a sum over the numbers of phonons that are emitted during the capture. The physical interpretation of these expressions is straightforward: field and temperature dependence of the carrier lifetimes are determined by the average of the carrier densities n and p with the product of the corresponding probability distributions, which originate from the quasi-exact treatment of the diagonal coupling terms of the Hamiltonian. The expressions (6) and (7) for the SRH lifetimes are very general; other recombination mechanisms could be described by simply replacing the multiphonon transition probability $M_{c,v}(l)$ by its equivalent.

The off-diagonal matrix elements enter the constants $\tau_{v,0}^{-1}$ which must be considered as fit parameters. Fortunately, we don't need them explicitly for our model. To see this, we "switch off" the field effect, i.e. we replace the tunneling probability $\mathcal{T}_v(l, x)$ by unity to get the inverse lifetimes $\hat{\tau}_v^{-1}(x, F = 0)$ for neutral regions. If we introduce these quantities into eqns (6) and (7), we can write

$$\hat{\tau}_v^{-1}(x) = \hat{\tau}_v^{-1}(x, F = 0) g_v[F(x)] \quad (8)$$

with field enhancement factors $g_v[F(x)]$

$$g_n[F(x)] = \frac{\sum_{l \geq 0} \rho_c^0(l) f_c(l) \mathcal{T}_c(l, x) M_c(l)}{\sum_{l \geq 0} \rho_c^0(l) f_c(l) M_c(l)}, \quad (9)$$

$$g_p[F(x)] = \frac{\sum_{l \geq 0} \rho_v^0(l)[1 - f_v(l)] \mathcal{T}_v(l, x) M_v(l)}{\sum_{l \geq 0} \rho_v^0(l)[1 - f_v(l)] M_v(l)}. \quad (10)$$

As eqns (9) and (10) show, these field enhancement factors again are given by mean values: the tunneling probability is averaged with the product of distribution function and multiphonon transition probability.

Now we can give the explicit expressions for $M_{c,v}(l)$ and $\mathcal{T}_{c,v}(l, x)$. As already indicated by the sums over phonon numbers, the Einstein model is used for the phonons, which means that the phonon spectrum of silicon is replaced by one effective mode with energy $\hbar\omega_0$. Such a treatment is standard in multiphonon theory to restrict the number of parameters to a minimum. On the other hand, it often seems to be just the local modes connected with the electronic defect that couple effectively to the bound carrier, which gives the use of the Einstein model a certain justification. Since energy can only be exchanged in amounts of a multiple of $\hbar\omega_0$, the effective phonon energy is the natural unit on the energy scale.

The multiphonon transition probability $M_v(l)$ for nonradiative transitions is given by

$$M_{c,v}(l) = \frac{(l \mp S)^2}{S} \exp[-S(2f_B + 1)] \times \exp\left(\frac{\hbar\omega_0}{2kT}\right) I_l(2S\sqrt{f_B(f_B + 1)}). \quad (11)$$

Here I_l labels the modified Bessel function of order l, $f_B = [\exp(\hbar\omega_0/kT) - 1]^{-1}$ is the Bose function, and S the Huang–Rhys factor, which is a measure of the coupling strength of the diagonal electron–phonon coupling. The upper sign in the prefactor refers to electrons, the lower to holes. This prefactor stands instead of unity in the case of radiative multiphonon transitions. It shows a certain artefact of the theory that will be discussed later. It can not be excluded that coupling strength and effective phonon energy have different values for the two different capture processes. We will assume that the difference between the thermal cross sections of electrons and holes is mainly due to the off-diagonal coupling terms, which determine the constants $\tau_{v,0}^{-1}$, and therefore, use the same values of S and $\hbar\omega_0$ for both capture processes.

effective mass, respectively. For hole tunneling we assumed that the hole tunneling mass m_v is isotropic. This mass must be regarded as the major uncertainty in the description of tunneling in semiconductors. Silicon has not only warped $E(k)$-surfaces, but degenerate bands of light and heavy holes at $k = 0$. A strong electric field will remove this degeneracy and change the curvature of the bands in the vicinity of the Γ-point. Since it is nearly impossible to calculate the consequences of this effect on the tunneling probability (see [38] for an attempt), we will use the value of the light hole mass ($m_{lh} = 0.16m_0$) in our model[39,40].

Inserting (12), (13) and Boltzmann factors for $f_{c,v}(l)$ into (9) and (10) gives for the field enhancement factors

$$g_n[F(x)] = \frac{\pi \sum\limits_{l \geqslant 0} (l - S)^2 \exp\left\{-\frac{l\hbar\omega_0}{2kT}\right\} I_l(z) \sum\limits_{i=x,y,z} \sqrt{\hbar\Theta_{i,\parallel}}\, \mathscr{F}\left(\frac{E_t - l\hbar\omega_0}{\hbar\Theta_{i,\parallel}}\right)}{3 \sum\limits_{l \geqslant \frac{E_t}{\hbar\omega_0}} (l - S)^2 \exp\left\{-\frac{l\hbar\omega_0}{2kT}\right\} I_l(z) \sqrt{l\hbar\omega_0 - E_t}}, \tag{14}$$

$$g_p[F(x)] = \frac{\pi \sum\limits_{l \geqslant 0} (l + S)^2 \exp\left\{-\frac{l\hbar\omega_0}{2kT}\right\} I_l(z) \sqrt{\hbar\Theta_v}\, \mathscr{F}\left(\frac{E_g - E_t - l\hbar\omega_0}{\hbar\Theta_v}\right)}{\sum\limits_{l \geqslant \frac{(E_g - E_t)}{\hbar\omega_0}} (l + S)^2 \exp\left\{-\frac{l\hbar\omega_0}{2kT}\right\} I_l(z) \sqrt{l\hbar\omega_0 - (E_g - E_t)}}. \tag{15}$$

The bound-to-band tunneling transitions are direct, first order processes due to the above mentioned delocalization of the bound state in k-space. The constant field approximation is used, which is much better fulfilled for trap tunneling than for band-to-band tunneling, again due to the strong localization of the bound state in real space. Therefore, the transition rate only depends on the local field strength at x. Apart from a field independent factor, the tunneling probability then is determined by

$$\mathscr{T}_c(l, x) = \sum_{i=x,y,z} \sqrt{\hbar\Theta_{i,\parallel}}\, \mathscr{F}\left(\frac{E_t - l\hbar\omega_0}{\hbar\Theta_{i,\parallel}}\right),$$

$$\mathscr{T}_v(l, x) = \sqrt{\hbar\Theta_v}\, \mathscr{F}\left(\frac{E_g - E_t - l\hbar\omega_0}{\hbar\Theta_v}\right). \tag{12}$$

In eqn (12) $\mathscr{F}$ denotes the electrooptical function $\mathscr{F}(y) = \mathrm{Ai}'^2(y) - y\mathrm{Ai}^2(y)$, and Θ_v the electrooptical frequency, $\Theta_v = (e^2F^2/2\hbar m_v)^{1/3}$. The mass $m_{i,\parallel}$ is the electron tunneling mass in field direction, which differs for the three pairs of equivalent conduction band valleys ($i = x, y, z$)

$$m_{i,\parallel} = \frac{m_t}{1 - (1 - m_t/m_l)F_i^2(x)/F^2(x)}. \tag{13}$$

$F_i(x)$ is the ith field component in a coordinate system with axes parallel to the [100]-directions. The masses m_t and m_l are the transverse and longitudinal

We have introduced the abbreviation

$$z = 2S\sqrt{f_B(f_B + 1)} \tag{16}$$

for the argument of the Bessel function.

The further calculation is performed only for $g_n[F(x)]$. Results can be immediately applied to $g_p[F(x)]$ by minor changes that are obvious from eqns (14) and (15).

The sum in the numerator of (14) is split into two partial sums below and above the band edge, respectively

$$\sum_{l \geqslant 0} = \sum_{\frac{E_t}{\hbar\omega_0} > l \geqslant 0} + \sum_{l \geqslant \frac{E_t}{\hbar\omega_0}}. \tag{17}$$

Because the asymptotic behaviour of the function $\mathscr{F}(y)$ for large negative arguments is given by

$$\lim_{y \to -\infty} \mathscr{F}(y) = \frac{1}{\pi}\sqrt{-y}, \tag{18}$$

the partial sum above the band edge in the numerator together with the denominator of eqn (14) tends to unity for vanishing electric field. For nonvanishing field the value is smaller than unity, since density of states is spread over the gap by the field. We take advantage of the fact that this deviation from unity is negligible for small field strengths and unimportant for large fields, where the enhancement factor be-

comes much greater than unity. Consequently, we can write for all field strengths

$$g_n[F(x)] = 1 + \tilde{g}_n[F(x)] \tag{19}$$

with

$$\tilde{g}_n[F(x)] = \frac{\pi \sum\limits_{\frac{E_t}{\hbar\omega_0} > l \geqslant 0} (l-S)^2 \exp\left\{-\frac{l\hbar\omega_0}{2kT}\right\} I_l(z) \sum\limits_{i=x,y,z} \sqrt{\hbar\Theta_{i,\parallel}}\, \mathscr{F}\left(\frac{E_t - l\hbar\omega_0}{\hbar\Theta_{i,\parallel}}\right)}{3 \sum\limits_{l \geqslant \frac{E_t}{\hbar\omega_0}} (l-S)^2 \exp\left\{-\frac{l\hbar\omega_0}{2kT}\right\} I_l(z) \sqrt{l\hbar\omega_0 - E_t}}. \tag{20}$$

We are now able to use approximate expressions for the tunneling probability at energies below the band edge, keeping the correct zero-field limits for g_n and $\tilde{g}_n$ [$g_n(0) = 1, \tilde{g}_n(0) = 0$].

3. SIMPLIFIED MODELS

The first basic assumption for a simplification of the field enhancement factor $\tilde{g}_n$, which has already been mentioned above, is

$$l \gg 1. \tag{21}$$

For the sum in the numerator of (20) this implies that transitions near or even at the trap level E_t must remain negligible. This is a constraint to the temperature and field strength and restricts the simplified model, roughly speaking, to the pre-breakdown range

This relation cannot be fulfilled, if the field strength is so small that the most contributing transitions occur close to the band edge, i.e. for those phonon numbers l^* which lead to $E_t - l^*\hbar\omega_0 \approx \hbar\Theta_{i,\parallel}$. On the other hand, (24) is related to the first condition (21).

Extremely large fields, which give an electrooptical energy $\hbar\Theta_{i,\parallel}$ comparable to the trap depth E_t (and therefore very small phonon numbers l^*) are excluded by (24) as well.

With (24) we may use the asymptotic form of the electrooptical function $\mathscr{F}$ for large positive arguments (WKB approximation)

$$\mathscr{F}\left(\frac{E_t - l\hbar\omega_0}{\hbar\Theta_{i,\parallel}}\right) \rightarrow \frac{1}{8\pi} \frac{\hbar\Theta_{i,\parallel}}{E_t - l\hbar\omega_0} \times \exp\left[-\frac{4}{3}\left(\frac{E_t - l\hbar\omega_0}{\hbar\Theta_{i,\parallel}}\right)^{3/2}\right]. \tag{25}$$

The denominator in the prefactor gives rise to a divergency, if the WKB approximation breaks down.

The field enhancement factor (20) becomes with (21)–(25)

$$\tilde{g}_n[F(x)] = \frac{\frac{1}{8}\int_0^{E_t} \mathrm{d}E(E - S\hbar\omega_0)^2 \exp\left(-\frac{E}{2kT}\right) I_{E/\hbar\omega_0}(z) \sum\limits_{i=x,y,z} \frac{(\hbar\Theta_{i,\parallel})^{3/2}}{(E_t - E)} \exp\left[-\frac{4}{3}\left(\frac{E_t - E}{\hbar\Theta_{i,\parallel}}\right)^{3/2}\right]}{3\int_{E_t}^{\infty} \mathrm{d}E(E - S\hbar\omega_0)^2 \exp\left(-\frac{E}{2kT}\right) I_{E/\hbar\omega_0}(z)\sqrt{E - E_t}} \tag{26}$$

at a given temperature. With the relation (21) we may replace the sums in (20) by integrals

$$\sum_l \rightarrow \frac{1}{\hbar\omega_0}\int \mathrm{d}(l\hbar\omega_0) \tag{22}$$

and use the asymptotic form of the modified Bessel function for large orders

$$I_l(z) \rightarrow \frac{1}{\sqrt{2\pi}} \frac{1}{(l^2 + z^2)^{1/4}} \exp(\sqrt{l^2 + z^2}) \times \exp\left(-l \ln\left[\frac{l}{z} + \sqrt{1 + l^2/z^2}\right]\right). \tag{23}$$

The second basic assumption excludes both too small and too strong electric fields

$$\frac{E_t - l\hbar\omega_0}{\hbar\Theta_{i,\parallel}} \gg 1. \tag{24}$$

where the asymptotic form (23) of $I_{E/\hbar\omega_0}(z)$ has to be inserted.

The integrand in the numerator is determined by the overlap of an exponentially decaying function originating from the decreasing multiphonon transition probability (the process is as less probable as more phonons are involved), and an exponentially rising function, which describes the increasing tunneling probability as the energy approaches the band edge. The resulting bell-shaped curve has its maximum between trap level and band edge. The position of that maximum, which we denote by E_0 in the following, is mainly determined by the exponential terms. It moves to the trap level with rising field strength or decreasing temperature (coupling strength), and it moves to the band edge with decreasing field strength or rising temperature (coupling strength). This maximum determines the most

probable transition energy, and therefore the most probable recombination path. Figure 1 illustrates the change of the recombination path with field strength.

The value of the field enhancement factor depends only weakly on the non-exponential terms, which justifies two further approximations. We have already mentioned that the factor $(E - S\hbar\omega_0)^2$ exhibits an artefact of the standard multiphonon theory[41]. If E equals the lattice relaxation energy $\epsilon_R = S\hbar\omega_0$, the probability of thermally induced transitions vanishes. This happens when in a configuration-coordinate diagram the lower potential parabola (bound state) crosses the upper parabola (band state) at its minimum. Then the lattice potential around the crossing point is completely anharmonic in contradiction to the requirements of first order perturbation theory. Extrinsic self-trapped centers[42] are a well known example. In a strong electric field the upper parabola is transformed into a continuum of such parabolas, which spread to lower energies with decreasing density, so that the described situation is always present at a transition energy $E = \epsilon_R$. As long as the lattice relaxation energy ϵ_R is small compared to the optimum transition energy E_0, the factor $(E - S\hbar\omega_0)^2$ is unproblematic. Nevertheless, we will replace it by unity, which actually means that the average (9) is performed with the line shape function only, i.e. without $(1 - S)^2/S$ in eqn (11). It is interesting to note that the factor does not appear in a two-phonon model[43], if one distinguishes between accepting and promoting modes.

The second approximation refers to the factor $(E_t - E)^{-1}$, which is related to the WKB approach (25). It strongly falsifies the tunneling probability at small field strengths, but has only little influence on the result in the pre-breakdown range. Therefore, we replace it by a mean value $2/E_t$.

Equation (26) then turns to

$$\tilde{g}_n[F(x)] = \sum_{i=x,y,z} \frac{(\hbar\Theta_{i,\parallel})^{3/2}}{4E_t} \int_0^{E_t} dE \left(1 + \left(\frac{E}{z\hbar\omega_0}\right)^2\right)^{-1/4} \exp\left\{\sqrt{\left(\frac{E}{\hbar\omega_0}\right)^2 + z^2} - \frac{E}{\hbar\omega_0} \ln\left[\frac{E}{z\hbar\omega_0} + \sqrt{1 + \left(\frac{E}{z\hbar\omega_0}\right)^2}\right]\right\} \times \exp\left(-\frac{E}{2kT}\right) \exp\left[-\frac{4}{3}\left(\frac{E_t - E}{\hbar\Theta_{i,\parallel}}\right)^{3/2}\right] \Big/ 3\int_{E_t}^{\infty} dE \left[1 + \left(\frac{E}{z\hbar\omega_0}\right)^2\right]^{-1/4} \exp\left\{\sqrt{\left(\frac{E}{\hbar\omega_0}\right)^2 + z^2} - \frac{E}{\hbar\omega_0} \ln\left[\frac{E}{z\hbar\omega_0} + \sqrt{1 + \left(\frac{E}{z\hbar\omega_0}\right)^2}\right]\right\} \exp\left(-\frac{E}{2kT}\right) \sqrt{E - E_t} \quad (27)$$

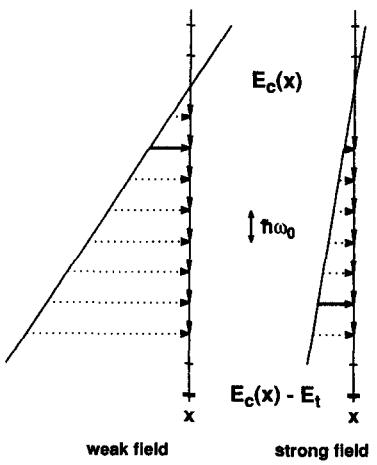

Fig. 1. Change of the most probable transition path with electric field strength. $E_c(x)$ denotes the conduction band edge at x, $E_c(x) - E_t$ is the trap energy level and $\hbar\omega_0$ the effective phonon energy.

In order to make the model suitable for device simulation, we must avoid numerical integrations. Hence, we evaluate the integrals analytically and then compare the approximate results with the "exact" expression (27). We will use the fact that the integrands are bell-shaped and fall off exponentially at both sides. Therefore, the stationary phase method can be applied. The exponent is developed up to second order around its maximum, which determines the transition energy E_0

$$J = \int_a^b dE \exp[f(E)],$$

$$f(E) \approx (E_0) + (E - E_0)f'(E_0) + \frac{(E - E_0)^2}{2} f''(E_0). \quad (28)$$

The transition energy E_0 is given by the zero of the first derivative of the exponent

$$f'(E_0) = 0. \quad (29)$$

If we extend the limits of the integral a and b to $-\infty$ and ∞, respectively, the integral J is approximately

$$J \approx \exp[f(E_0)] \int_{-\infty}^{\infty} dE \exp\left[\frac{(E - E_0)^2}{2} f''(E_0)\right] = \exp[f(E_0)] \sqrt{\frac{2\pi}{|f''(E_0)|}}. \quad (30)$$

The main problem is to find the root E_0 of eqn (29) which we need for the approximate solution (30). To solve that problem we examine two usual approaches of multiphonon theory—the high and low temperature approximation.

3.1. *High temperature approximation*

The integrals in the numerator and denominator of expression (27) for the field enhancement factor are determined by a thermal weight function

$$W(E) = [E^2 + (z\hbar\omega_0)^2]^{-1/4} \exp\left\{\sqrt{\left(\frac{E}{\hbar\omega_0}\right)^2 + z^2} - \frac{E}{\hbar\omega_0} \ln\left[\frac{E}{2\hbar\omega_0} + \sqrt{1 + \left(\frac{E}{z\hbar\omega_0}\right)^2}\right] - \frac{E}{2kT}\right\} \quad (31)$$

with z defined in eqn (16). In the high temperature approximation one assumes

$$z^2 \gg \left(\frac{E}{\hbar\omega_0}\right)^2, \quad z \to 2S\frac{kT}{\hbar\omega_0}. \quad (32)$$

The thermal weight function (31) then becomes

$$W(E) = \frac{\exp\left(\frac{2SkT}{\hbar\omega_0} + \frac{\epsilon_R}{4kT}\right)}{\sqrt{2SkT}} \exp\left[-\frac{(E+\epsilon_R)^2}{4\epsilon_R kT}\right] \quad (33)$$

with the lattice relaxation energy $\epsilon_R = S\hbar\omega_0$. If we insert this into eqn (27), we get for the field enhancement factor

Here we have denoted with E^0_{act} the activation energy for capturing an electron from the conduction band edge (see Fig. 2): $E^0_{act} = (E_t - \epsilon_R)^2/4\epsilon_R$. Now, using (30) and (37)–(39) in eqn (34), the field enhancement factor in the high temperature approximation can be written as

$$\tilde{g}_n[F(x)] = \frac{1}{3}\sum_{i=x,y,z}\left(1 + \frac{2\epsilon_R kT}{(\hbar\Theta_{i,\parallel})^{3/2}\sqrt{E_t - E_0}}\right)^{-1/2} \times \frac{E^0_{act} + E_t}{kT}\left(\frac{\hbar\Theta_{i,\parallel}}{E_t + \epsilon_R}\right)^{3/2} \times \exp\left\{\frac{E^0_{act} - E_{act}(F)}{kT}\right\}\exp\left\{\frac{E_t - E_0}{kT}\right\} \times \exp\left\{-\frac{4}{3}\left(\frac{E_t - E_0}{\hbar\Theta_{i,\parallel}}\right)^{3/2}\right\}, \quad (40)$$

with E_0 given by eqn (35) and $E_{act}(F) = (E_0 - \epsilon_R)^2/4\epsilon_R$. The pre-breakdown behaviour is caused by the interplay of the three exponential factors. Their physical meaning is easily understood. The first exponent contains the difference of the activation energies for electron capture without and with electric field, respectively. A rising electric field lowers the effective activation energy for carrier capture, since the effective trap depth for the thermal (vertical) transition is no longer E_t but $E_0 < E_t$. We illustrate both activation energies in Fig. 2. The second exponent describes an increase of occupation probability as the trap depth is effectively lowered by

$$\hat{g}_n[F(x)] = \frac{\sum_{i=x,y,z}\frac{(\hbar\Theta_{i,\parallel})^{3/2}}{4E_t}\int_0^{E_t} dE \exp\left\{-\frac{(E+\epsilon_R)^2}{4\epsilon_R kT}\right\}\exp\left\{-\frac{4}{3}\left(\frac{E_t - E}{\hbar\Theta_{i,\parallel}}\right)^{3/2}\right\}}{3\int_{E_t}^{\infty} dE \exp\left\{-\frac{(E+\epsilon_R)^2}{4\epsilon_R kT}\right\}\exp[\tfrac{1}{2}\ln(E - E_t)]}. \quad (34)$$

We first calculate the integral in the numerator. The root (29) can be found analytically and gives for the transition energy as a function of field strength and temperature

$$E_0 = 2\sqrt{\epsilon_F}[\sqrt{\epsilon_F + E_t + \epsilon_R} - \sqrt{\epsilon_F}] - \epsilon_R \quad (35)$$

where we have used the abbreviation

$$\epsilon_F = \frac{(2\epsilon_R kT)^2}{(\hbar\Theta_{i,\parallel})^3}. \quad (36)$$

The second derivative of the exponent which is responsible for the fall-off of the integrand, turns out to be

$$f''(E_0) = -\frac{1}{2\epsilon_R kT} - \frac{1}{(\hbar\Theta_{i,\parallel})^{3/2}\sqrt{E_t - E_0}} \quad (37)$$

where both terms can have the same order of magnitude. If we proceed with the denominator as with the numerator, we get for the zero-field transition energy E^0_0, for the exponent $g(E)$ of the integrand and its second derivative

$$E^0_0 \approx E_t + \frac{\epsilon_R kT}{E_t + \epsilon_R}, \quad (38)$$

$$g(E^0_0) \approx -\frac{E^0_{act}}{kT} - \frac{E_t}{kT} + \frac{1}{2}\ln\left(\frac{\epsilon_R kT}{E_t + \epsilon_R}\right), \quad g''(E^0_0) \approx -\frac{1}{2}\left(\frac{E_t + \epsilon_R}{\epsilon_R kT}\right)^2. \quad (39)$$

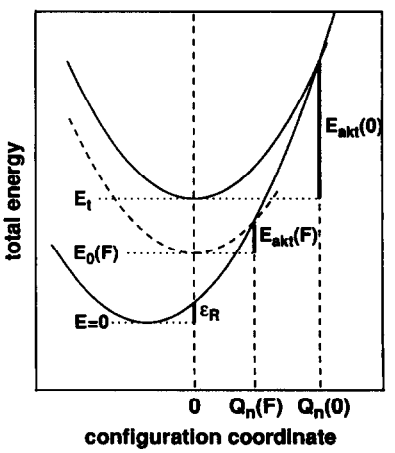

Fig. 2. Lowering of the activation energy in a strong electric field. Q_n denotes the crossing points of the adiabatic potential parabolas (electron capture), ϵ_R is the lattice relaxation energy.

the electric field. The last exponential is the well known tunneling factor for the penetration of a triangular barrier, but with a field dependent tunneling depth $\Delta = E_t - E_0$ measured from the conduction band edge (compare Fig. 1).

It should be mentioned that the result for hole capture follows from (40), if E_t is replaced by $E_g - E_t$, $\Theta_{i,\parallel}$ by Θ_v, and ϵ_R by the corresponding value for hole capture. The advantage of the high temperature approximation is, besides its physical transparency, that only two parameters of the recombination center are necessary for each lifetime—the energy level, and the lattice relaxation energy. The drawback is the well known fact that the prerequisite (32) actually holds "after the crystal has already smelted". We will discuss the quality of the high temperature approximation in the next subsection.

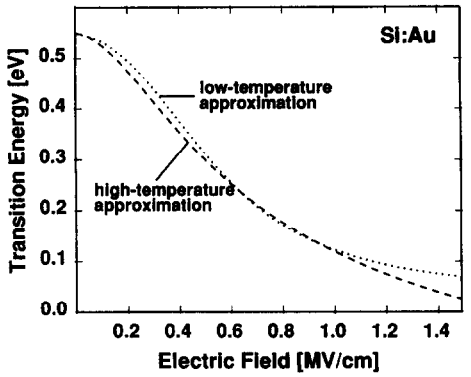

Fig. 3. Transition energy, measured from the trap level, as function of the electric field. Parameters: $E_t = 0.55$ eV, $S = 3.5$, $\hbar\omega_0 = 0.068$ eV, $T = 300$ K.

3.2. *Low temperature approximation*

In contrast to (32) the low temperature approximation is defined by

$$z^2 \ll \left(\frac{E}{\hbar\omega_0}\right)^2, \quad z \to 2S\exp\left(-\frac{\hbar\omega_0}{2kT}\right). \tag{41}$$

The thermal weight function now takes the form

$$W(E) = E^{-1/2}\exp\left(\frac{E}{\hbar\omega_0} - \frac{E}{kT}\right) \times \exp\left[-\frac{E}{\hbar\omega_0}\ln\left(\frac{E}{\epsilon_R}\right)\right]. \tag{42}$$

Inserting into eqn (27) gives for the field enhancement factor

$$\tilde{g}_n[F(x)] = \frac{\sum_{i=x,y,z}\dfrac{(\hbar\Theta_{i,\parallel})^{3/2}}{4E_t}\displaystyle\int_0^{E_t} dE E^{-1/2}\exp\left\{-\frac{E}{kT} + \frac{E}{\hbar\omega_0}\left[1 - \frac{E}{\hbar\omega_0}\ln(E/\epsilon_R)\right] - \frac{4}{3}\left(\frac{E_t - E}{\hbar\Theta_{i,\parallel}}\right)^{3/2}\right\}}{3\displaystyle\int_{E_t}^{\infty} dE E^{-1/2}\exp\left\{-\frac{E}{kT} + \frac{E}{\hbar\omega_0}\left[1 - \frac{E}{\hbar\omega_0}\ln(E/\epsilon_R)\right] + \frac{1}{2}\ln(E - E_t)\right\}}. \tag{43}$$

We again use the exponential term to determine the most probable transition energy E_0. The factor $E^{-1/2}$ is pulled out of the integral at this energy. The same is done in the denominator. The root of the first derivative of the exponent in the numerator now is solution of the implicit equation

$$\frac{2kT}{(\hbar\Theta_{i,\parallel})^{3/2}}\sqrt{E_t - E_0} = 1 + \frac{kT}{\hbar\omega_0}\ln\left(\frac{E_0}{\epsilon_R}\right). \tag{44}$$

There is no satisfactory approximate solution to this equation in the field strength range of interest. The numerical solution for E_0 as function of field strength is shown in Fig. 3, using parameters of the gold acceptor in silicon[36,37,44,45], and is compared there with the result of the high temperature approximation (35). A serious discrepancy is observed only beyond about 1.2 MV/cm, but there the validity of the basic assumption (21) already starts to fail, i.e. we must consider this field strength as the end of the pre-breakdown range. Hence, because there is no significant difference for the function $E_0(F)$ in both approximations, we can avoid the iteration of eqn (44), and use the analytical solution (35) instead. For the second derivative of the upper exponent we get

$$f''(E_0) = -\frac{1}{E_0\hbar\omega_0} - \frac{1}{(\hbar\Theta_{i,\parallel})^{3/2}\sqrt{E_t - E_0}}. \tag{45}$$

The zero-field transition energy E_0^0 in the denominator is also solution of an implicit relation

$$1 = 2\frac{E_0^0 - E_t}{\hbar\omega_0}\left[\frac{\hbar\omega_0}{kT} + \ln\left(\frac{E_0^0}{\epsilon_R}\right)\right]. \tag{46}$$

A sufficient approximate root that is in agreement with the low temperature approach, is

$$E_0^0 \approx E_t + \frac{kT}{2}. \tag{47}$$

Exponent and second derivative at this energy are given then by

$$g(E_0^0) \approx \frac{E_t + kT/2}{\hbar\omega_0} - \frac{E_t + kT/2}{kT} + \frac{1}{2}\ln\left(\frac{kT}{2E_t}\right) - \frac{E_t}{\hbar\omega_0}\ln\left(\frac{E_t}{\epsilon_R}\right), \quad g''(E_0^0) \approx -\frac{2}{(kT)^2}. \tag{48}$$

If (30), (45), (47) and (48) are inserted into (43), the field enhancement factor in low temperature approximation becomes

$$\tilde{g}_n[F(x)] = \frac{1}{3}\sum_{i=x,y,z}\left(1 + \frac{(\hbar\Theta_{i,\parallel})^{3/2}\sqrt{E_t - E_0}}{E_0\hbar\omega_0}\right)^{-1/2} \times \frac{(\hbar\Theta_{i,\parallel})^{3/4}(E_t - E_0)^{1/4}}{2\sqrt{E_t E_0}}\left(\frac{\hbar\Theta_{i,\parallel}}{kT}\right)^{3/2}$$

$$\times \exp\left\{-\frac{E_t - E_0}{\hbar\omega_0} + \frac{\hbar\omega_0 - kT}{2\hbar\omega_0} + \frac{E_t + kT/2}{\hbar\omega_0} \times \ln(E_t/\epsilon_R) - \frac{E_0}{\hbar\omega_0}\ln(E_0/\epsilon_R)\right\} \times \exp\left(\frac{E_t - E_0}{kT}\right)\exp\left[-\frac{4}{3}\left(\frac{E_t - E_0}{\hbar\Theta_{i,\parallel}}\right)^{3/2}\right]. \quad (49)$$

The structure of that formula is quite similar to the result in the high temperature approximation. If we compare the three exponentials, we notice that only the first one is different. The activation law of the high temperature approximation is replaced by a less transparent factor depending not only on the lattice relaxation energy alone, but explicitly on the effective phonon energy.

In Fig. 4 we compare the field enhancement factors of electron lifetimes, calculated in the different models with parameters of the gold acceptor in silicon. The dashed line represents the high temperature approximation [eqn (40)], the dotted curve is the result of the low temperature approximation [eqn (49)], and the solid curve originates from the "exact" expression (27), where the integrals have been calculated numerically using the original asymptotic form of the Bessel function (23). The agreement of the low temperature approach with the "exact" curve is excellent over the whole range of field strength, but even the high temperature approximation reproduces the general course quite well. The reason for the deviation of the latter is the strong violation of the precondition $kT \gg \hbar\omega_0$ for the example Si–Au ($kT = 0.0258$ eV, $\hbar\omega_0 = 0.068$ eV).

Because of the good agreement we will use eqn (49) for the further discussion.

4. TEMPERATURE DEPENDENCE OF ZERO-FIELD LIFETIMES

In order to study the temperature dependence of the SRH lifetimes, we must know the temperature behaviour of their zero-field part $\hat{\tau}_v(x, F = 0)$ [compare eqn (8)]. We go back to the general expression (6) for the electron lifetime (the expressions for hole lifetimes are straightforward)

$$\hat{\tau}_n^{-1}(x, F = 0) = \tau_{n,0}^{-1} N_t(x) \frac{1}{N_c} \sum_{l \geq 0} \rho_c^0(l) M_c(l) \times \exp\left(\frac{E_t - l\hbar\omega_0}{kT}\right) \quad (50)$$

where we have inserted the Boltzmann factor for the distribution function and replaced the tunneling probability by unity. We assume that the off-diagonal matrix element, which is contained in $\tau_{n,0}^{-1}$, does only weakly depend on temperature, so that we can neglect this effect. We also neglect a possible temperature dependence of the trap energy level E_t. Then we may proceed as in the previous section and use the high and low temperature approximation, respectively.

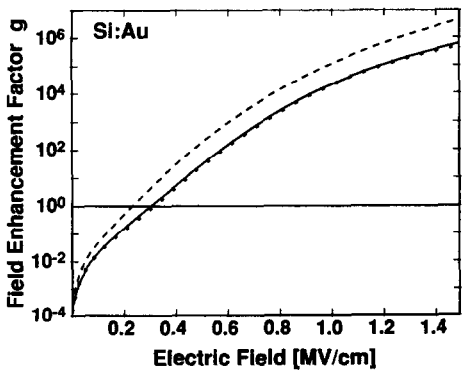

Fig. 4. Field enhancement factor as function of electric field in different approximations: high temperature approximation (dashed curve), low temperature approximation (dotted curve), and "exact" eqn (27) (solid curve). For parameters see Fig. 3.

4.1. High temperature approximation

Retaining only the temperature dependent factors and using (33), we get

$$\hat{\tau}_n^{-1}(T) \sim \frac{1}{\sqrt{T}} \exp\left(\frac{E_t}{kT} + \frac{\epsilon_R}{4kT}\right) \int_{E_t}^{\infty} dE \times \exp\left[-\frac{(E + \epsilon_R)^2}{4\epsilon_R kT}\right] \exp[\tfrac{1}{2}\ln(E - E_t)], \quad (51)$$

and with (37)–(39)

$$\hat{\tau}_n^{-1}(T) \sim T \exp\left(-\frac{E_{act}^0}{kT} + \frac{\epsilon_R}{4kT}\right). \quad (52)$$

Equation (52) shows that in the high temperature approximation the zero-field lifetimes are thermally activated. Taking 300 K as reference temperature, we may write finally

$$\hat{\tau}_n(T) = \hat{\tau}_n(300)\left(\frac{300}{T}\right) \times \exp\left[\frac{(E_{act}^0 - \epsilon_R/4)}{kT}\left(1 - \frac{T}{300}\right)\right]. \quad (53)$$

4.2. Low temperature approximation

A better approximation is to use (42) in (50). Retaining again only the temperature dependent factors, we have

$$\hat{\tau}_n^{-1}(T) \sim \exp\left(\frac{E_t}{kT}\right) \int_{E_t}^{\infty} dE E^{-1/2} \times \exp\left\{-\frac{E}{kT} + \frac{E}{\hbar\omega_0}\left[1 - \frac{E}{\hbar\omega_0}\ln(E/\epsilon_R)\right] + \tfrac{1}{2}\ln(E - E_t)\right\}. \quad (54)$$

Proceeding as in the previous section, i.e. using (47) and (48), the temperature dependence of the inverse zero-field lifetime becomes

$$\hat{\tau}_n^{-1}(T) \sim T^{3/2} \exp\left\{\frac{kT}{2\hbar\omega_0}[1 - \ln(E_t/\epsilon_R)]\right\}. \quad (55)$$

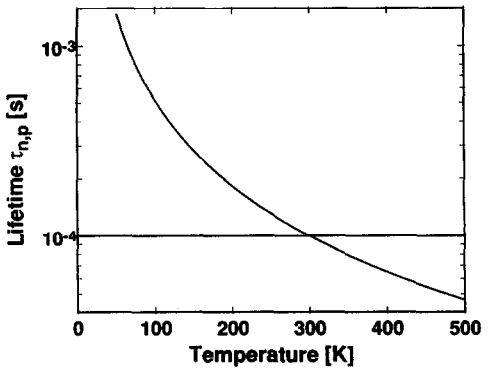

Fig. 5. Temperature dependence of zero-field electron lifetime in the low temperature approximation. $\tau_n = 10^{-4}$ s has been assumed for $T = 300$ K.

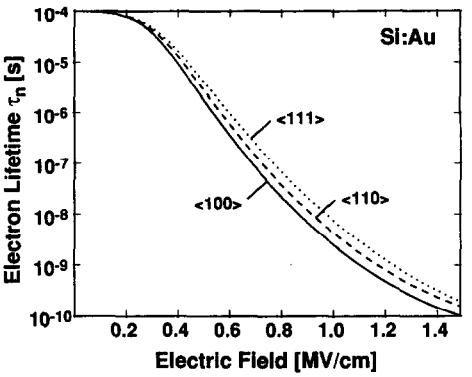

Fig. 7. Electron lifetime as function of the electric field for different field orientations. For parameters see Fig. 3.

The exponential factor can be neglected, since $kT \ll \hbar\omega_0$ in accordance with the low temperature approach. Thus, we get finally

$$\hat{\tau}_n(T) = \hat{\tau}_n(300)\left(\frac{300}{T}\right)^{3/2}. \tag{56}$$

The result is plotted in Fig. 5. As the temperature goes down, the zero-field SRH lifetimes increase, since the probability of thermal capture decreases. Whereas in the high temperature approach this effect is thermally activated, the temperature dependence in the low temperature approximation is much weaker. The $T^{3/2}$-law should be much more realistic in silicon than the activation law (53), at least for the example under consideration.

5. RESULTS AND DISCUSSION

The further discussion will also be based on the extensively studied gold acceptor in silicon[45]. We use for the trap level $E_t = 0.55$ eV, for the Huang–Rhys factor $S = 3.5$, and for the effective phonon energy $\hbar\omega_0 = 0.068$ eV. The latter value was suggested by Mott *et al.*[46], and is close to the optical phonon energy. No temperature dependence of the thermal cross section was found[45], which supports the large value of $\hbar\omega_0$. Using this value, Morante *et al.*[47] obtained a Huang–Rhys factor of 2.2–2.6.

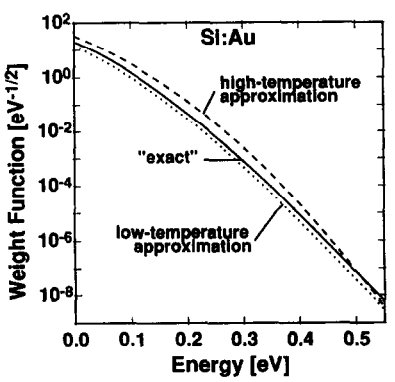

Fig. 6. Comparison of the different approximations for the thermal weight function $W(E)$. For parameters see Fig. 3.

In [37] it was shown that the best fit to DLTS data in a two-phonon model with accepting and promoting modes gives the larger value $S \approx 3.5$. Because we have neglected the square of the crossing point $(l \mp S)^2/S$ in (11), in agreement with the consequences of two different phonon modes, we also use $S = 3.5$ here.

The field dependence of the SRH lifetimes is well described by field enhancement factors (8), calculated in the low temperature approximation of multiphonon theory [eqn (49)]. Despite the approximate analytical solution of the convolution integrals, and despite the approximate form of the multiphonon transition probability, the agreement with the more general factor (including numerical integration and a more exact thermal weight) is surprisingly good, as shown in Fig. 4. This can be understood, if the three expressions for the thermal weight function $W(E)$ are compared among each other. We plotted these functions over the energy range between trap level and band edge in Fig. 6. Obviously, the deviation of the high temperature result for the field enhancement factor is caused by the rather strong deviation of the corresponding thermal weight function (33) from the "exact" one (31). Near the band edge all three curves coincide. Thus, the overlap with the zero-field density of states must result in equal values, independent of the applied approximation, giving also the same value for the denominator in the ratio which determines the field enhancement factor. On the other hand, the size of the field effect is determined by the numerator, which is overestimated by the thermal weight function of the high temperature approximation.

The anisotropy of the field effect of the electron lifetime is illustrated in Fig. 7. A lifetime of 10^{-4} s was chosen as the zero-field limit at room temperature. The numerical values for the tunneling mass follow from (13). In Table 1 we arranged the expressions for the resulting masses in ⟨100⟩-, ⟨110⟩-, and ⟨111⟩-direction. Using $m_t = 0.19m_0$ and $m_l = 0.92m_0$ one obtains $m_{\langle 110\rangle} = 0.315m_0$ and $m_{\langle 111\rangle} = 0.258m_0$. The field enhancement is dominated by the pair of valleys with the smallest mass. Thus, one could drop the term with $m_{x,\parallel}$ in the case of ⟨100⟩-direction, and the two

Table 1. Electron tunneling masses for different orientations of the electric field

		$i = x$	$i = y$	$i = z$
⟨100⟩	F_i^2/F^2	1	0	0
	$m_{i,\parallel}$	m_l	m_t	m_t
⟨110⟩	F_i^2/F^2	1/2	1/2	0
	$m_{i,\parallel}$	$2\left[\frac{1}{m_t}+\frac{1}{m_l}\right]^{-1}$	$2\left[\frac{1}{m_t}+\frac{1}{m_l}\right]^{-1}$	m_t
⟨111⟩	F_i^2/F^2	1/3	1/3	1/3
	$m_{i,\parallel}$	$3\left[\frac{2}{m_t}+\frac{1}{m_l}\right]^{-1}$	$3\left[\frac{3}{m_t}+\frac{1}{m_l}\right]^{-1}$	$3\left[\frac{2}{m_t}+\frac{1}{m_l}\right]^{-1}$

terms with $m_{x,\parallel}, m_{y,\parallel}$ in the case of ⟨110⟩-direction, respectively. Figure 7 shows that the maximum difference between the two extrema ⟨100⟩ and ⟨111⟩ is about a half order of magnitude only. In the light of the assumptions made so far and the uncertainty caused by the trap parameters, this difference is rather small. The reasons for that are the six conduction band valleys of silicon, which effectively average the tunneling probability.

The temperature dependence of the field enhanced electron lifetime is shown in Fig. 8 using the $T^{-3/2}$-law [eqn (56)] for the zero-field limits. As expected, there is a pronounced increase of the field effect at lower temperatures. This emphasizes the crucial importance of bound-to-band tunneling transitions at operating temperature of liquid nitrogen (LN_2). On the other hand, the range of validity of our model is further restricted when the temperature goes down, since the optimum transition energy E_0 approaches the trap level, and the precondition $l \gg 1$ (21) fails.

An important point for the applicability of the model is the number and availability of the parameters. The supposed model (49) with E_0 given by eqn (35), based on the low temperature approach, contains the following characteristic energies:

kT—thermal energy
$\hbar\Theta_v$—electrooptical energy
E_t—trap energy level
ϵ_R—lattice relaxation energy
$\hbar\omega_0$—effective phonon energy
$E_0 = E_0(\hbar\theta_v, \epsilon_R, E_t, kT)$—optimum transition energy.

The first energy is given by the temperature, the last one is only a function of the others. The electrooptical energy $\hbar\Theta_v = (e^2\hbar^2F^2/2m_v)^{1/3}$ is defined by the field strength $F(x)$ and the tunneling mass m_v. Hence, this energy is also given, apart from the uncertainty concerning the correct effective mass m_v for the tunneling holes. The three remaining energies E_t, ϵ_R, and $\hbar\omega_0$ are (in principle) available by DLTS for each kind of recombination centers. If nothing else is known about the nature of the traps, one has to proceed in a practical way. E_t should be replaced by $E_g/2$ then, because mid-gap centers are most efficient in recombination. The two remaining (physical) parameters $\epsilon_R = S\hbar\omega_0$ and $\hbar\omega_0$, which are characteristic for an individual recombination center, may serve as fit parameters. Realistic values for silicon are: $\hbar\omega_0 \approx 0.065$ eV, $\epsilon_R \sim$ [100–300] meV.

It is interesting to study the influence of ϵ_R and $\hbar\omega_0$ on the field dependence of the lifetimes. We showed above that in the high temperature approximation the result [see eqn (40)] only depends on ϵ_R, while $\hbar\omega_0$ does not occur explicitly. Hence, it is to be expected that even in the low temperature approach the result does not vary very strongly with $\hbar\omega_0$, if $\epsilon_R = S\hbar\omega_0$ is kept constant. This is illustrated in Fig. 9. Keeping the lattice relaxation energy constant at a value of 240 meV, and decreasing the phonon energy from 60 to 24 meV results in a steeper course of the pre-breakdown, but the maximum difference is not much more than one order of magnitude.

The lattice relaxation energy ϵ_R has the major influence on the field effect of the lifetimes, as shown

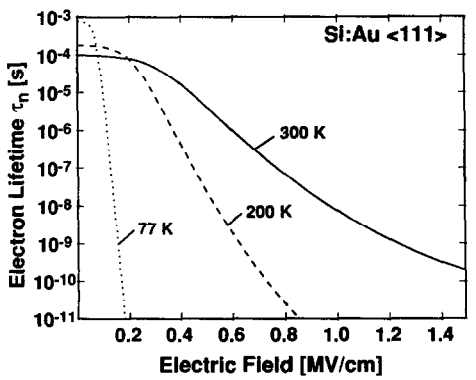

Fig. 8. Electron lifetime as function of the electric field in ⟨111⟩-direction for different temperatures. For parameters see Fig. 3.

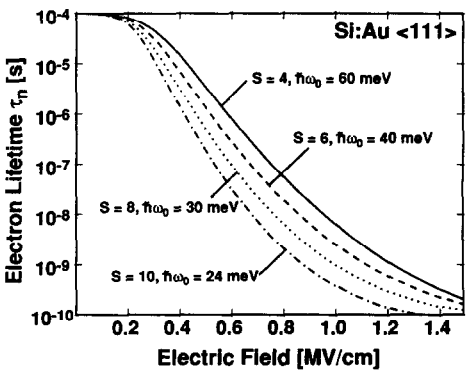

Fig. 9. Electron lifetime as function of the electric field in ⟨111⟩-direction for constant lattice relaxation eenrgy ϵ_R, but different Huang–Rhys factor S and effective phonon energies $\hbar\omega_0$. $T = 300$ K.

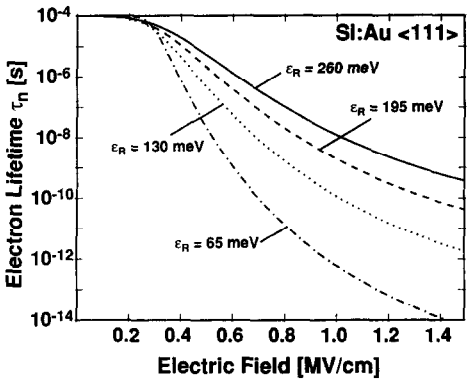

Fig. 10. Electron lifetime as function of the electric field in ⟨111⟩-direction for different lattice relaxation energies ϵ_R. $T = 300$ K.

in Fig. 10. As the electron-phonon coupling becomes weaker, ϵ_R decreases, and the lifetimes decrease faster with rising field strength. The onset of the field effect between 0.2 and 0.3 MV/cm is independent of the center parameters. Decreasing ϵ_R has the same effect as decreasing temperature, therefore, the above made remark on the range of validity of the model also holds for the lattice relaxation energy.

To conclude, the derived model for the field and temperature dependence of SRH lifetimes is a useful tool for the calculation of bound-to-band tunneling leakage phenomena in silicon devices. Because of its analytical simplicity it is suitable for the implementation into device simulation programs. The three physical parameters of the model (E_t, ϵ_R, and $\hbar\omega_0$), which are necessary to describe the recombination center and the coupling of its electronic wave function of the lattice, may be reduced to actually one crucial parameter (ϵ_R), if no detailed information about the nature of the recombination centers is available.

REFERENCES

1. A. Schenk, *J. appl. Phys.* **71,** 3339 (1992).
2. J. C. S. Woo, J. D. Plummer and J. M. C. Stork, *IEEE Trans. Electron Devices* **ED-34,** 130 (1987).
3. J. A. del Alamo and R. M. Swanson, *IEEE Electron Device Lett.* **EDL-7,** 629 (1986).
4. G. A. M. Hurkx, D. B. M. Klaassen, M. P. G. Knuvers and F. G. O'Hara, *IEDM Tech. Digest*, p. 307 (1989).
5. G. Vincent, A. Chantre and D. Bois, *J. appl. Phys.* **50,** 5484 (1979).
6. S. H. Voldman, J. B. Johnson, T. D. Linton and S. L. Titcomb, *IEDM Tech. Digest* 349 (1990).
7. W. Shockley and W. T. Read Jr, *Phys. Rev.* **87,** 835 (1952); R. N. Hall, *Phys. Rev.* **87,** 387 (1952).
8. J. Frenkel, *Phys. Rev.* **54,** 647 (1938).
9. K. Huang and A. Rhys, *Proc. R. Soc. Lond.* **A204,** 406 (1950); K. Huang, *Scienta Sinica* **XXIV,** 27 (1981).
10. M. A. Krivoglaz, *Zh. Eksper. Theor. Fiz.* **25,** 191 (1953).
11. G. Helmis, *Ann. Phys.* **19,** 41 (1956).
12. Yu. E. Perlin, *Fiz. Tverd. Tela* **2,** 242 (1960).
13. C. H. Henry and D. V. Lang, *Phys. Rev.* **B15,** 989 (1977).
14. R. Pässler, *Czech. J. Phys.* **B24,** 322 (1974); **B25,** 219 (1975); *Physica status solidi* (b) **85,** 203 (1978).
15. B. K. Ridley, *Solid-St. Electron.* **21,** 1319 (1978).
16. M. G. Burt, *J. Phys.* **C6,** 4137 (1983).
17. K. Peuker, R. Enderlein, A. Schenk and E. Gutsche, *Physica status solidi* (b) **109,** 599 (1982).
18. A. Schenk, D. Suisky and R. Enderlein, *Acta phys. polonica* **A71,** 315 (1987).
19. W. Franz, *Z. Naturf.* **13a,** 484 (1958); L. V. Keldysh, *Zh. Eksper. Teor. Fiz.* **34,** 1138 (1958).
20. W. V. Houston, *Phys. Rev.* **57,** 184 (1940).
21. E. N. Adams, *J. chem. Phys.* **21,** 2013 (1953).
22. L. V. Keldysh, *Sov. Phys. JETP* **6,** 763 (1958); **7,** 665 (1958).
23. E. O. Kane, *J. Phys. Chem. Solids* **12,** 181 (1959).
24. P. J. Price, *Bull. Am. Phys. Soc.* **5,** 406 (1960).
25. E. O. Kane, *J. appl. Phys.* **32,** 83 (1961).
26. C. B. Duke and M. E. Alferieff, *Phys. Rev.* **145,** 583 (1965).
27. D. E. Aspnes, *Phys. Rev.* **147,** 554 (1966).
28. D. E. Aspnes, F. A. Germano and P. Handler, *Phys. Rev.* **166,** 921 (1968).
29. R. Enderlein, R. Keiper and W. Tausenfreund, *Physica status solidi* **33,** 69 (1969).
30. D. F. Blossey, *Phys. Rev.* **B2,** 3976 (1970); **B3,** 1382 (1970).
31. V. S. Vinogradov, *Fiz. Tverd. Tela* **13,** 3266 (1971).
32. R. Enderlein and K. Peuker, *Physica status solidi* (b) **48,** 231 (1971).
33. H. Köster Jr, O. V. Kurnusova and I. N. Yassievich, *Physica status solidi* (b), **127,** 339 (1984).
34. A. Schenk, M. Stahl and H.-J. Wünsche, *Physica status solidi* (b) **154,** 815 (1989).
35. S. Makram-Ebeid and M. Lannoo, *Phys. Rev.* **B25,** 6406 (1982).
36. A. Schenk, K. Irmscher, D. Suisky, R. Enderlein, F. Bechstedt and H. Klose, *Proc. 17th ICPS*, San Francisco (edited by J. C. Chadi and W. A. Harrison), p. 613. Springer, Berlin (1984).
37. A. Schenk, Ph.D. Thesis, Humboldt-University, Berlin (1986).
38. R. Enderlein, P. Renner and M. Scheele, *Physica status solidi* (b) **71,** 503 (1975).
39. P. Lawaetz, *Phys. Rev.* **B4,** 3460 (1971).
40. S. M. Sze, *Physica of Semiconductor Devices*, 2nd edn. Wiley, New York (1981).
41. E. Gutsche, *Physica status solidi* (b) **109,** 583 (1982).
42. I. Toyozawa, *Solid-St. Electron.* **21,** 1316 (1978).
43. A. Schenk, R. Enderlein and D. Suisky, *Acta phys. polonica* **A69,** 813 (1986).
44. A. F. Tasch and C. T. Sah, *Phys. Rev.* **B1,** 800 (1970).
45. D. V. Lang, H. G. Grimmeis, E. Meijer and M. Jaros, *Phys. Rev.* **B22,** 3917 (1980).
46. N. Mott, E. A. Davis and H. A. Street, *Phil. Mag.* **32,** 961 (1975).
47. J. R. Morante, J. E. Carceller, P. Cartujo and J. J. Barbolla, *Physica status solidi* (b) **111,** 375 (1982).